Estimation of high temperature mechanical properties of CrN and CrAlN coatings from *in-situ* Synchrotron Radiation X-ray Diffraction

Ehsan Mohammadpour[§], Zhong-Tao Jiang[§,*], Mohmmednoor Altarawneh[§,*] Zonghan Xie[⊥], Zhi-feng Zhou[$], Nicholas Mondinos[§], Justin Kimpton[±], Bogdan Z. Dlugogorski[§],

[§]School of Engineering & Information Technology, Murdoch University, Murdoch, WA 6150, Australia.

[⊥]School of Mechanical Engineering, University of Adelaide, SA 5005, Australia

[$]Department of Mechanical and Biomedical Engineering, City University of Hong Kong, Kowloon, Hong Kong, China

[±]Australian Synchrotron, 800 Blackburn Rd., Clayton, VIC 3168, Australia

Abstract

This contribution investigates the phase composition of CrN and CrAlN coatings by *in-situ* high temperature synchrotron radiation (SR-XRD), with the coatings deposited on steel substrate by closed field unbalance magnetron sputtering. Rietveld refinement on the SR-XRD spectra indicated CrN as the major phase, over the temperature range of 25 °C – 700 °C, for both coatings. At the high temperature of 700 °C, a Cr_2N phase was observed in the CrN coating while the CrAlN coating also had a Cr phase. Williamson-Hall plots, from the refined data, afforded estimating variations of the strain and crystallite size of the major phase, up to 700 °C. The crystallite size (10 nm) for the CrAlN coating, at 25 °C, agrees very well with previous GI-XRD and TEM results obtained at room temperature [1].

Keywords: hard coatings, strain, Williamson-Hall, synchrotron radiation, high temperature X-ray diffraction, Rietveld refinement, GSASII,

Corresponding author:

Tel.: +61 8 9360 2867; Email address: Z.Jiang@murdoch.edu.au (Z.-T. Jiang)

Tel.: +61 8 9360 7507; Email address: M.Altarawneh@murdoch.edu.au (M. Altarawneh)

Introduction

Magnetron-sputtered hard-surface coatings composed of transition metal nitride have been utilised to improve the productivity of cutting machinery in a wide range of applications such as drills, mills and cutting tools [2][3][4]. The main merit of magnetron sputtering is the attainment of robust control of the composition and microstructure of hard films and other nanostructured composite materials [5].

Due to their exceptionally high hardness characteristics and outstanding wear resistance, TiN coatings are major component in cutting machinery. However, TiN coatings exhibit only moderate resistance to oxidation and corrosion lessening their duration of use. In contrast CrN coatings display enhanced performance under oxidative and corrosive conditions that is primarily derived from the formation of an isolating adhesive chromium oxide layer on the coated surface [6]. In some applications, the thickness of film coating is an important parameter in deciding the type of coating to use. The maximum thickness of TiN coatings is typically limited to 10 μm, while CrN coatings can be made with thicknesses of more than 40 μm [7]. However, CrN coatings are associated with significantly lower hardness (*i.e.* 12.0 – 18.0 GPa), compared with TiN coatings (> 20 GPa). The demand for improved properties has resulted in development of ternary and multinary coatings such as CrAlN, CrAlYN, CrSiN, CrAlSiN and CrAlTiN [8].

Incorporating (alloying) Al in the cubic lattice of c-CrN coatings forms a metastable phase that considerably improves the hardness of the coating. Since c-CrN exhibits high solubility for c-AlN, ternary CrAlN nanocomposite coatings are promising pseudo binary nitrides in which Al and Cr sesquioxides provide effective resistance against oxygen diffusion through the coating [9]. Outward diffusion of Cr and Al ions, to the surface in CrAlN coatings, results in the formation of complex surface oxides which enhance the thermal properties of CrAlN by acting as barriers against further oxidation [5]. Additionally the hardness and thermal stability of CrAlN is enhanced by Al substitution of Cr atoms in the face-centred cubic structure of c-CrN [8]. The solute atoms are believed to hinder slip by diffusing to and segregating around dislocations [10]. These two hardness-enhancing mechanisms in coatings are determined by the Al content and are characterised by formation of a metastable solid solution that produces internal lattice strains. Properties of such coating are highly sensitive to Al content where

excessive addition of Al beyond 64 at. % changes the structure from rock-salt (NaCl) crystal structure (Fm3m) to wurtzite structure (P-31m) resulting in deterioration of hardness and anti-oxidation properties with alteration of preferred growth orientation [11]. Formation of hexagonal h-AlN structures significantly decreases hardness and thermal stability of CrN coatings reducing the benefit of Al alloying [12].

High temperature properties of hard coatings primarily depend on their crystalline-phase structures. Alloying elements, present in the phase formed during the deposition stage, exert a noticeable influence on the durability and the expected service life of hard coatings [13]–[19]. Any significant variations in grain size of coatings may affect their thermal stability [20]. Therefore, any unforeseen changes in microstructure and phase composition of coating material can potentially reduce the thermal resistance and hardness [21] of the coatings. Since coatings deposited by the sputtering techniques are in a non-equilibrium condition [22], it is of vital importance to study the microstructure of the coatings at elevated temperatures.

Literature articles and reviews discuss overall mechanical and thermal properties including various preparation techniques of CrAlN coatings, in terms of their microstructure [23], effects of atomic ratio (*i.e.* Al/Cr ratios) on their phase composition [2][24], deposition control parameters [25], [26], and high temperature oxidation properties [18], [19].

Tribological properties of CrN coatings with Al and Si dopants deposited by cathodic arc, studied by Polcar *et al.* [27], showed high hardness, excellent oxidation resistance and thermal stability up to 800 °C. X-ray analysis showed that, the dominant structure in Al and Si-doped coating material was cubic solid solution of Al in CrN. However, hexagonal AlN was also detected in the AlCrSiN coating. Sánchez-López *et al*. [12] studied the tribological behaviour of CrAl(Y,Zr)N coatings at 300, 500 and 650 °C, and concluded that the CrAlN coating had lower film wear due to high hardness and presence of Al_2O_3 on the coating surface. Forsen *et al*. [28] reported improved hardness of CrAlN coating by addition of Ti which improves the formation of h-AlN at annealing temperatures up to 1100 °C. The enhanced hardness was due to spinodal decomposition into coherent TiCr and Al-rich structures of the coating material, causing age hardening that stabilised the significantly improved hardness. Wang *et al*. [18] deposited CrN and CrAlN using single electron beam plasma assisted physical vapour deposition (PAPVD) system, annealed them at 500 °C-1000 °C and then cooled down to 25 °C for characterisation. Their analysis showed orthorhombic CrN structure in the CrN coating, CrN was converted to β-Cr_2N at about 500 °C and Cr_2O_3 was detected above 700 °C. A solid

solution of (Cr,Al)N was detected in the CrAlN coating and was stable up to 900 °C. The hardness of CrN coating dropped from 24.8 GPa to 16 GPa at 600 °C. On the other hand, the original hardness of CrAlN amounted to 30 GPa which decreased to 21.6 GPa after annealing at 600 °C. CrAlN solid solutions can be deposited with up to 66.0 at.% of Al input [29][15], which precipitates into a more stable h-AlN phase with low mechanical properties, above 800 °C, as a result of a spinodal reaction [30].

Kirchlechner *et al*. [31] studied the deposition of CrN coating by reactive magnetron sputtering at temperatures of 25 °C – 850 °C. They employed high intensity synchrotron radiation beamline to obtain diffraction spectra from both coating and steel substrate simultaneously which enabled determination of strains and internal stresses of the coating and the substrate. Rivadulla *et al*. [32] used synchrotron radiation (λ = 0.44397 Å) in combination with *ab initio* calculations to identify the cubic to orthorhombic transformation of CrN at pressures of about 1 GPa. This transformation reduces the bulk modulus of the coatings.

The promising properties of CrAlN coatings highly depend on their complex phase behaviour and more detailed studies on their nanostructure could lead to fabrication of improved hard coatings. In our previous studies [2] [1], we employed multiple surface and subsurface analysis characterisation techniques to investigate $Cr_xAl_{1-x}N$ coatings on various substrates. Results revealed the formation of CrAlN solid solution, with amorphous AlN present at columnar CrN grain boundaries. The next step necessitates an accurate investigation of the role of Al on the change of crystal structure phases of CrN coatings at temperatures up to 700 °C. We explore the phase composition and crystal structure of the aforementioned coating in the temperature range of 25 °C to 700 °C using *in-situ* SR-XRD measurements. Finally, we analysed the SR-XRD measurements to predict of the crystallite size and strain of the main phases up to 700 °C

Experimental procedure

CrAlN coatings were deposited on M2 high speed steel substrates using closed field unbalanced magnetron sputtering system (Teer Coatings Ltd, UK) with four-target configuration. The coating process has been described in detail elsewhere [1][33]. To observe a phase formation in the CrAlN coatings, *in-situ* SR-XRD measurements were carried out as a function of temperature. Synchrotron radiation has a number of advantages including the ability to tune the wavelength to avoid the formation of sample fluorescence, superior energy bandpass and significantly higher signal/noise (S/N) compared to a laboratory instrument. The experiment was performed on the Powder Diffraction beamline at the Australian Synchrotron with

monochromated X-rays of wavelength 0.82647 Å. The X-ray diffraction data were collected on a Mythen microstrip detector and the wavelength was determined by Rietveld refinement of a Standard Reference Material, LaB6 660b, as supplied by the National Institute of Standards and Technology (USA). The coated substrates were mounted on a Pt heating strip in an Anton Paar HTK-2000 high temperature furnace and aligned to the centre of rotation on the diffractometer. The samples were heated from ambient temperature up to 700 °C with heating rate of 10 °/min and X-ray diffraction data were collected over the angular range $10° \leq 2\theta \leq 89°$. The sample surface temperature was calibrated before experiment.

Samples made with CrN coating on M2 steel will be denoted as CrN-M2ST and samples made with $Cr_xAl_{1-x}N$ coating on M2 steel will be denoted as CrAlN-M2ST.

Theoretical procedure

In the present study, assuming Bragg-Brentano geometry, phase analysis of SR-XRD data was performed by the Rietveld method using the GSASII software package [34]. Initially refinement was applied to the unit cell parameter while all other structural parameters were fixed to the original standard values of the JCPDF data files listed in the results and discussion section. The crystal strain, atomic position, atomic isotropic temperature, zero shift, background as Chebyshev polynomial of fifth degree, peak profile, sample displacement and texture were then successively refined. The fittings were performed using analytic Hessian refinement derivatives. These corrections help to obtain physically realistic intensities, displacement and peak width models when analysing diffraction patterns in non-standard geometries.

Results and discussions

The coating composition was analysed at room temperature by X-ray Photoelectron Spectroscopy (XPS) [1] and the results are listed in Table 1.

Table 1. Contents of coating sample obtained from XPS measurements

	Concentration at. %			
Samples	Cr	Al	N	O
CrAlN-M2ST	27.5	14.2	31.8	26.6
CrN-M2ST	49.6	-	30.3	20.1

The phases found in the coatings, from SR-XRD, are: CrN (JCPDF 011-0065), AlN (JCPDS 046-1200), Al (JCPDS 004-0787), Cr_2N (JCPDS 00-035-0803), Cr (JCPDS 00-900-8467) and AlO_2 (JCPDS 00-901-1413) on a substrate of Fe (JCPDS 006-0696) dominated M2 steel. For clarity, only the Miller indices of appropriate phases are indicated in the SR-XRD plots of Figures 1-3. Peaks without Miller indices are due to the M2 steel substrate.

Figure 1 (a) and (b) shows the SR-XRD patterns for CrN coating (18° – 30° 2θ range) and CrAlN coatings (18° – 27° 2θ range) respectively, at 25, 200, 500, 600 and 700 °C. The emphasis is on the CrN, AlN, Al, Cr_2N and Cr phases.

(a)

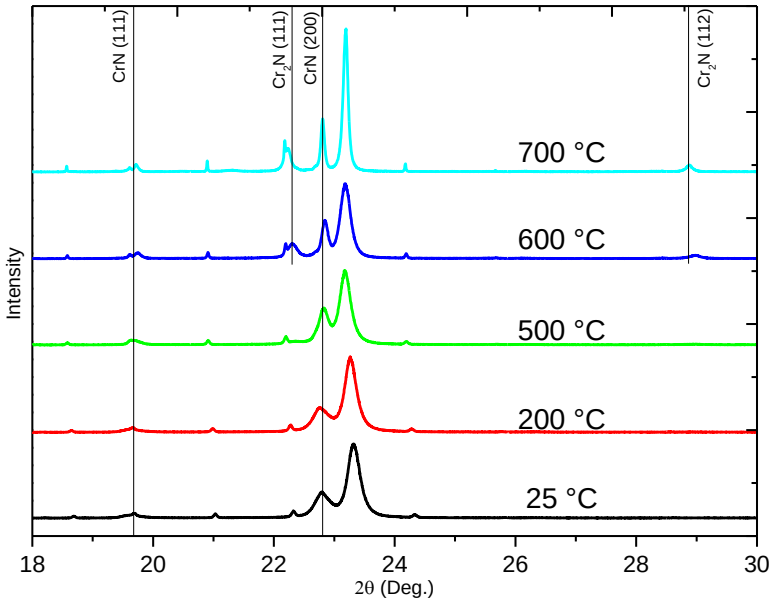

(b)

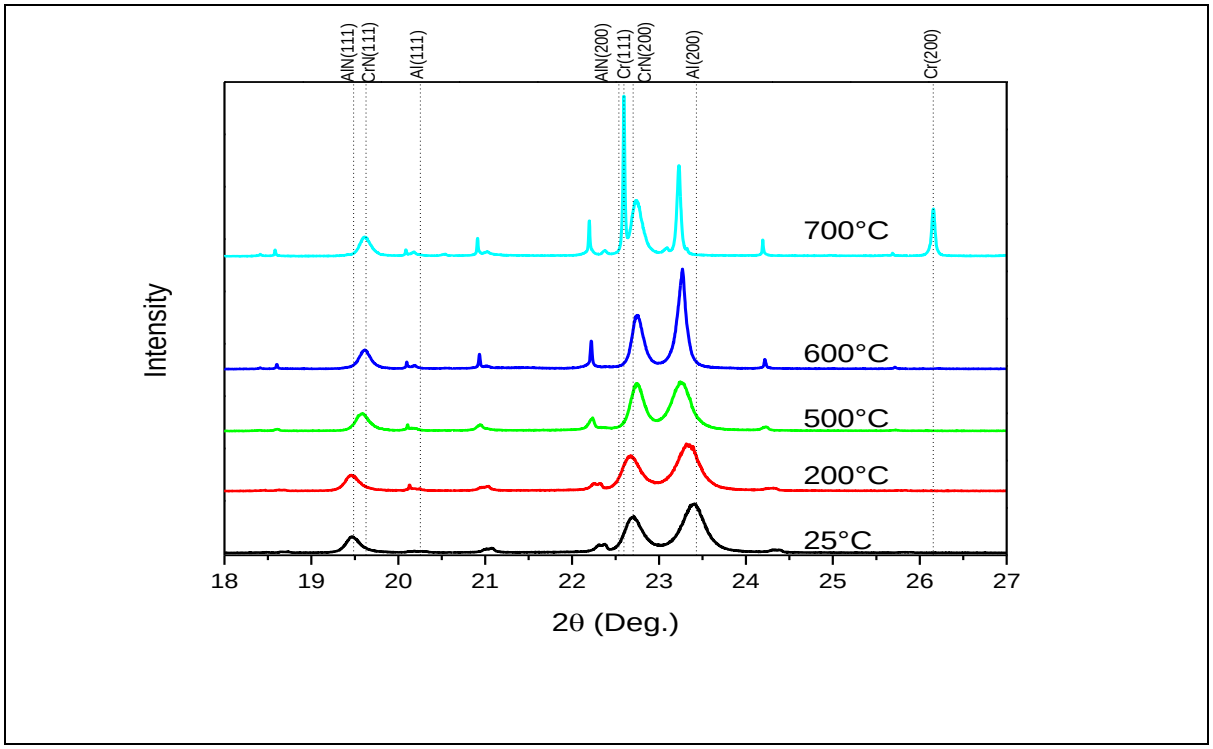

Figure 1. SR-XRD patterns of (a) CrN-M2ST and (b) CrAlN-M2ST samples at different temperatures

For the CrN-M2ST samples, CrN is the main phase over the entire temperature range with a Cr_2N phase produced above 600 °C. For the CrAlN-M2ST samples, CrN is a major phase over the entire temperature range. A cubic AlN phase is observed up to 500 °C. From 600 °C the c-AlN phase disappears. Due to the similar crystal structure of CrN and c-AlN phases, it is possible that they form a solid solution, as there is a shift of peaks in the diffraction pattern of CrN with increasing temperature. It is also possible that, the grain size of AlN has become very small and undetectable by XRD. Above 600 °C, a significant Cr phase and a very small amount of AlO_2 phase appear. Lu *et al.* [39] have investigated Aluminium peroxide (AlO_2) formation in the interfacial region of Pt-Al_2O_3 (sapphire) couple (≈ 1mm plates). It's interesting that the authors state that formation of AlO_2 occurs in the range of 1200 °C to 1400 °C but not below 1100 °C.

The room temperature XPS results indicate the appearance of oxygen for both samples. The Cr2p3/2 and Cr2p1/2 bonding states of CrAlN-M2ST sample indicate a combination of CrN and Cr_2O_3 on the surface. The Al2p peak indicated a combination of AlN and Al_2O_3 on the surface. The N1s spectra consisted of a CrN component (strong peak) and a Cr-O-N component (weak peak). The binding energy of formation of Al_2O_3 and Cr_2O_3 oxides in the very top atomic layers of the surface can explain most of the detected oxygen [35]. Oxidation of CrN at high

temperatures occurs through outward diffusion of chromium, aluminium and nitrogen while oxygen diffuses inwardly and forms oxides inside coating layers [36], [37]. The formation of Cr-O-N was discussed by Minami et al. [38] which crystalized in similar cubic structure of CrN with strong diffraction in (111) and (200) directions. CrN coating material exhibits remarkable oxidation resistance due to its fine and dense equiaxial crystal structure which reduces the oxygen diffusion rate significantly. Formation of sticky aluminium and chromium oxides on the surface also hinder oxygen diffusion. Combination of these effects can restrict the formation of oxides only on very top surface layers which can be detected by XPS. There were no signs of Al_2O_3 and Cr_2O_3 phases in the SR-XRD results of CrAlN—M2ST samples below 600°C. However, small amounts of AlO_2 (≈2.8%) were formed between 600 °C and 700 °C.

CrN phase, with a rock-salt (NaCl) like unit cell, dominated the structure of the coating film. The crystallographic characteristic of coating was determined from refined synchrotron data. Results showed a significant change of the CrN lattice parameter in the CrAlN coating. The lattice parameter value of reference for the CrN phase was 4.145 Å (JCPDF 011-0065). Refinement of the lattice parameter resulted in a value of 4.209 Å at room temperature (25 °C) continuously decreasing to 4.167 Å at 600 °C and then abruptly increasing to 4.176 Å at 700 °C. The initial decrease of the lattice parameter, from room temperature value, can be attributed to the formation of a solid solution of Al/CrN from the diffusion of Al (from the cubic AlN and amorphous Al that is in the grain boundaries) into the CrN structure substituting the Cr atoms. The smaller size of Al atoms effectively reduces the lattice constant of the dominant phase in CrAlN. The TEM images of similar coating, discussed by Munroe *et al.* [1] and Rahman *et al.* [2], generated from cross section of the columnar CrN grains confirmed the presence of amorphous AlN phase between CrN grains, at room temperature. The continuous decline of unit cell value may indicate two simultaneous phenomena: (1) the higher amount of Al dissolution in the structure and (2) strain release due to temperature increment. CrN showed high solubility of Al which improves mechanical properties of coating material through the formation of a solid solution [9].

A major change in microstructure of CrAlN-M2ST samples occurred at the temperature range above 600 °C with the appearance of Cr diffraction peaks of substantial intensity and AlO_2 diffraction peaks of very low intensity. Results suggest that, the CrAlN coating (CrN/AlN grains and amorphous boundaries) produced a CrN-Cr/AlN-Cr multi-phase grain composition by crystallisation of Cr from the boundary into the grain due to thermal activation and Al from

the amorphous boundary forming AlO_2. It should be noted that, there is much less Al/AlN within the grains than in the amorphous boundaries.

Figure 2 depicts the refined SR-XRD pattern of the CrAlN-M2ST sample at 700 °C with emphasis on the main Cr, AlO_2 diffraction peaks. Main differences between experimental and fitted plots were due to the substrate peaks which are identified as a combination of Fe and Fe3W3C phases. Formation of metallic Cr and AlO_2 at 700 °C in the nanocomposites coating may indicate initiation of changes in mechanical properties of the film coating. Protective nanocomposite coatings can only preserve their hardness and mechanical properties provided the nanostructure remains stable and unchanged.

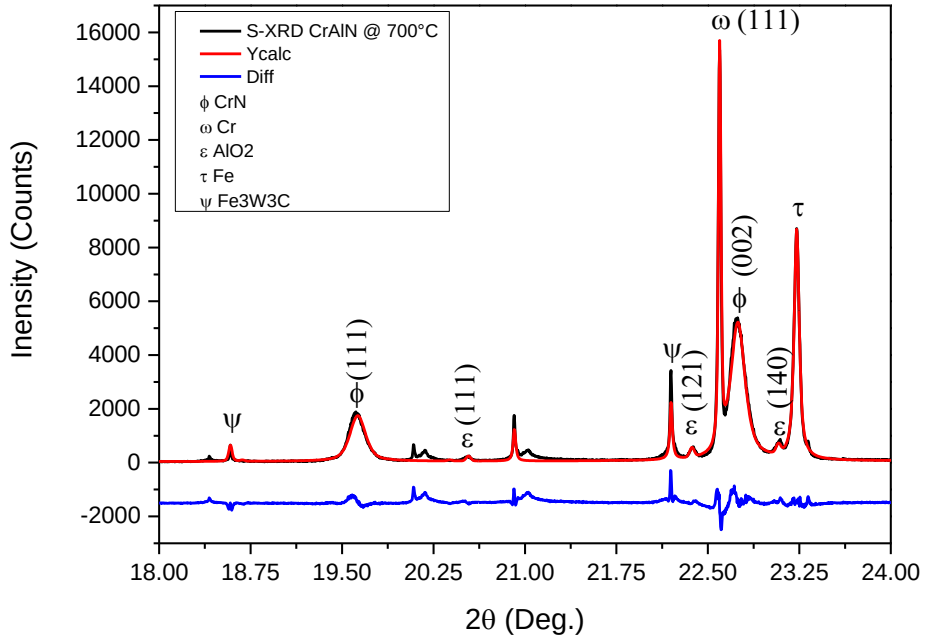

Figure 2. Refined SR-XRD pattern of CrAlN coating at 700 °C

Careful analysis of diffraction patterns in Figures 1 and 2 reveals changes in peak positions and widths as the temperature increased to 700 °C. Such shifts in peak positions and widths usually indicate change in lattice parameter and/or strain in the crystal structure. The high resolution refined SR-XRD data of the CrN and (Cr,Al)N phases are analysed to give some indication of the domain/crystallite sizes and strains in both the CrN-M2ST and CrAlN-M2ST samples, respectively, over the 25 °C – 700 °C temperature range. The same analysis is performed for the Cr phase at 700 °C.

The crystallite domain size and lattice strain are deduced from the Williamson-Hall equation [36]:

$$\text{Williamson-Hall equation:} \quad \beta\, cos\theta = 4\varepsilon\, sin\theta + \frac{K\lambda}{D} \qquad (1)$$

Where β, ε, D are the full width at half maximum, microstrain and domain/crystallite size, respectively. K is a constant which equals to 0.89 and λ is the X-ray wavelength [32]. GSAS refinement produced data of (hkl), d, 2θ and FWH values for all of the identified phases in the samples. This data is used to make plot of $\beta \cdot cos\theta$ *and* $4sin\theta$ (see figure 3).

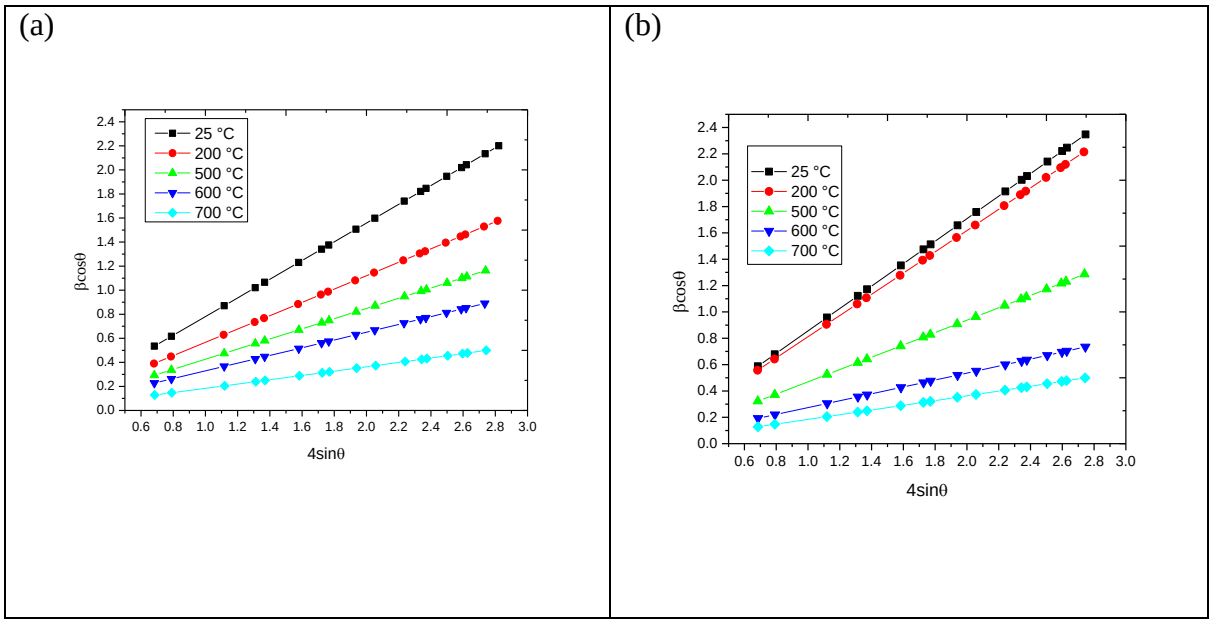

Figure 3. Williamson-Hall plots for CrN phase in (a) CrN-M2ST and (b) CrAlN-M2ST samples at different temperatures.

According to equation 1, the strain component (ε) is calculated from the slope and the crystallite domain size (D) from the intercept ($K\lambda/D$) at each temperature. The strain and domain/crystallite size of the CrN phase in CrN-M2ST and CrAlN-M2ST samples were estimated up to 700 °C and results shown in table 2 and figure 4.

Similar estimates of the strain and crystallite size for the Cr phase at 700 °C indicate crystallite size ≈ 11 nm and strain ≈ 0.001

Table 2. Calculated strain and crystallite size of CrN phase in the CrN-M2ST and CrAlN-M2ST samples at different temperatures (T)

T (°C)	Strain		Crystallite size (nm)	
	CrN-M2ST	CrAlN-M2ST	CrN-M2ST	CrAlN-M2ST
25	0.853	0.779	40.1	9.8
200	0.807	0.556	42.0	10.5
500	0.469	0.423	54.7	45.1
600	0.263	0.323	56.5	55.4
700	0.180	0.180	61.8	56.8

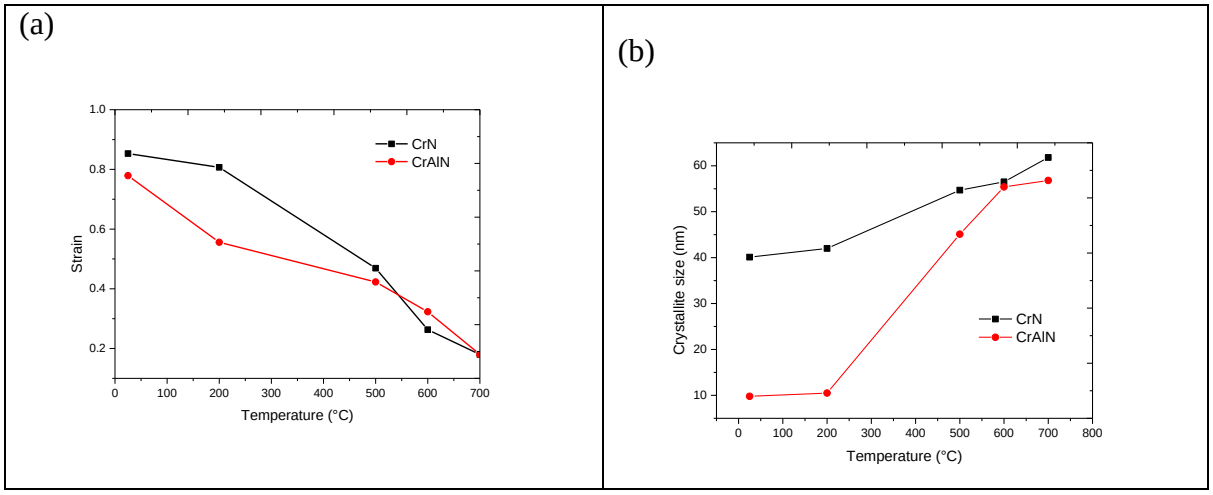

Figure 4 Calculated (a) strains *vs*. *T* and (b) crystallite size *vs.* T for CrN phase in the CrN-M2ST and CrAlN-M2ST samples

The plots of figure 4(b) indicate that, the crystallite sizes of the CrN phase are smaller in the CrAlN-M2ST samples than in the CrN-M2ST samples at all temperature. Furthermore, sizes increase as temperatures approach 700 °C, for both coatings. Previous room temperature GI-XRD and TEM studies of the same CrAlN-M2ST samples showed the size of crystallite domains of approximately 10 nm, in good agreement with current SR-XRD result at 25 °C [4]. Interestingly, the size of crystallites corresponds to about 11 nm at the high temperature of 700 °C, which is about the same size of the CrN crystallites in CrAlN-M2ST sample up to 200 °C.

The plots of figure 4(a) indicate the strain for the CrN phase follows a similar pattern with the crystallite size variation. The strains are less in the CrAlN-M2ST samples than in the CrN-

M2ST samples. Similarly, the strain decreases as the temperature increases up to 700 °C for both sample coatings. Since the Cr phase occurs above 600 °C, its strain value is unimportant.

The solid solution of AlN into CrN generally increases the strains of the lattice in bulk sized material. However thin films synthesised in plasma may not follow the general trend due to the complicated plasma process. These include very fast reaction and grain growth of the thin films at very short time periods. The direction of plasma and resulting equilibrium interactions add to the complication of the thin film growth mechanism. The higher strain results of CrN phase in the CrN-M2ST samples than in the CrAlN-M2ST samples are most probably due to the differing plasma interactions occurring at film coating synthesis. Interestingly at 600 °C and above the values for strain and crystallite size for the CrN phase in both samples are the same (within experimental errors). This could be due to the AlO_2 and Cr formation at that temperature range.

The calculated strain and size values imply that, the mechanical properties (such as hardness, elastic modulus) of the coatings deteriorate as the temperature increases from 25 °C – 700 °C. However measuring strains, hardness and grain sizes at very high temperatures is very challenging and in some cases probably impossible.

Conclusions

Rietveld analysis of *in-situ* high temperature synchrotron radiation X-ray diffraction (SR-XRD) of CrN and CrAlN coatings, deposited on M2 steel substrate by closed field unbalance magnetron sputtering, revealed CrN, Cr_2N, AlN, Al and Cr phases in the coatings. Analysis indicated that CrN is the major phase in both coatings at all temperatures. At the high temperature of 700 °C, formation of CrN, Cr and AlO_2 (~2.8%) phases in the CrAlN coatings were detected. Similarly Cr_2N phase was detected in the CrN coating.

Williamson-Hall plots were used to estimate the crystallite size and strains of the CrN phase for temperatures up to 700 °C. Analysis indicates a decrease in crystallite size and strains of the major phase, in both coatings, over the temperature range. The strains and crystallite size of the CrN phase in the CrAlN coating are less than those in the CrN coating for temperatures below 600 °C while they are equal above 600 °C. An estimate for the Cr phase indicated very

small crystallites of ~ 11 nm at 700 °C. The estimate crystallite size of ~ 10 nm at 25 °C, of CrN phase, for the CrAlN coating agrees well with previous TEM results.

Acknowledgment

This study has been supported by School of Engineering and Information Technology at Murdoch University. The authors gratefully acknowledge support provided by the Australian Synchrotron beam time award AS141/PD/7582. E. M greatly appreciates Murdoch University for the award of a postgraduate scholarship.

References

[1] Z. Li, P. Munroe, Z. Jiang, X. Zhao, J. Xu, Z. Zhou, J. Jiang, F. Fang, and Z. Xie, "Designing superhard, self-toughening CrAlN coatings through grain boundary engineering," *Acta Mater.*, vol. 60, no. 16, pp. 5735–5744, 2012.

[2] M. Mahbubur Rahman, A. Duan, Z.-T. Jiang, Z. Xie, A. Wu, A. Amri, B. Cowie, and C.-Y. Yin, "Near-edge X-ray absorption fine structure studies of Cr1−xMxN coatings," *J. Alloys Compd.*, vol. 578, pp. 362–368, Nov. 2013.

[3] J. Deng, F. Wu, Y. Lian, Y. Xing, and S. Li, "Erosion wear of CrN, TiN, CrAlN, and TiAlN PVD nitride coatings," *Int. J. Refract. Met. Hard Mater.*, vol. 35, pp. 10–16, Nov. 2012.

[4] F. L. M. Diserens, J. Patscheider, "Mechanical properties and oxidation resistance of nanocomposite TiN – SiN physical-vapor-deposited thin films," vol. 121, pp. 158–165, 1999.

[5] Y. Lv, L. Ji, X. Liu, H. Li, H. Zhou, and J. Chen, "The structure and properties of CrAlN films deposited by mid-frequency unbalanced magnetron sputtering at different substrate bias duty cycles," *Surf. Coatings Technol.*, vol. 206, no. 19–20, pp. 3961–3969, May 2012.

[6] J. Lin, W. D. Sproul, and J. J. Moore, "Microstructure and properties of nanostructured thick CrN coatings," *Mater. Lett.*, vol. 89, pp. 55–58, 2012.

[7] H. C. Barshilia, N. Selvakumar, B. Deepthi, and K. S. Rajam, "A comparative study of reactive direct current magnetron sputtered CrAlN and CrN coatings," *Surf. Coatings*

Technol., vol. 201, no. 6, pp. 2193–2201, Dec. 2006.

[8] M. Schlögl, J. Paulitsch, J. Keckes, and P. H. Mayrhofer, "Influence of AlN layers on mechanical properties and thermal stability of Cr-based nitride coatings," *Thin Solid Films*, vol. 531, pp. 113–118, 2013.

[9] Y. Makino and K. Nogi, "Synthesis of pseudobinary Cr-Al-N films with B1 structure by rf-assisted magnetron sputtering method," *Surf. Coatings Technol.*, vol. 98, no. 1–3, pp. 1008–1012, Jan. 1998.

[10] M. Benkahoul, P. Robin, S. C. Gujrathi, L. Martinu, and J. E. Klemberg-Sapieha, "Microstructure and mechanical properties of Cr-Si-N coatings prepared by pulsed reactive dual magnetron sputtering," *Surf. Coatings Technol.*, vol. 202, pp. 3975–3980, 2008.

[11] J. Lin, B. Mishra, J. J. Moore, and W. D. Sproul, "Microstructure, mechanical and tribological properties of Cr1−xAlxN films deposited by pulsed-closed field unbalanced magnetron sputtering (P-CFUBMS)," *Surf. Coatings Technol.*, vol. 201, no. 7, pp. 4329–4334, Dec. 2006.

[12] J. C. Sánchez-López, a. Contreras, S. Domínguez-Meister, a. García-Luis, and M. Brizuela, "Tribological behaviour at high temperature of hard CrAlN coatings doped with Y or Zr," *Thin Solid Films*, vol. 550, pp. 413–420, Jan. 2014.

[13] S. Zhang, L. Wang, Q. Wang, and M. Li, "A superhard CrAlSiN superlattice coating deposited by multi-arc ion plating: I. Microstructure and mechanical properties," *Surf. Coatings Technol.*, vol. 214, pp. 160–167, Jan. 2013.

[14] A. Rizzo, L. Mirenghi, M. Massaro, U. Galietti, L. Capodieci, R. Terzi, L. Tapfer, and D. Valerini, "Improved properties of TiAlN coatings through the multilayer structure," *Surf. Coatings Technol.*, vol. 235, pp. 475–483, Nov. 2013.

[15] R. Forsén, M. P. Johansson, M. Odén, and N. Ghafoor, "Effects of Ti alloying of AlCrN coatings on thermal stability and oxidation resistance," *Thin Solid Films*, vol. 534, no. 534, pp. 394–402, 2013.

[16] R. Forsén, M. Johansson, M. Odén, and N. Ghafoor, "Decomposition and phase transformation in TiCrAlN thin coatings," *J. Vac. Sci. Technol. A Vacuum, Surfaces, Film.*, vol. 30, no. 6, p. 061506, 2012.

[17] Z. B. Qi, B. Liu, Z. T. Wu, F. P. Zhu, Z. C. Wang, and C. H. Wu, "A comparative study of the oxidation behavior of Cr2N and CrN coatings," *Thin Solid Films*, vol. 544, pp. 515–520, Oct. 2013.

[18] L. Wang and X. Nie, “Effect of Annealing Temperature on Tribological Properties and Material Transfer Phenomena of CrN and CrAlN Coatings,” *J. Mater. Eng. Perform.*, vol. 23, no. 2, pp. 560–571, Oct. 2013.

[19] S. Mato, G. Alcalá, M. Brizuela, R. Escobar Galindo, F. J. Pérez, and J. C. Sánchez-López, “Long-term high temperature oxidation of CrAl(Y)N coatings in steam atmosphere,” *Corros. Sci.*, vol. 80, pp. 453–460, Mar. 2014.

[20] A. Raveh, I. Zukerman, R. Shneck, R. Avni, and I. Fried, “Thermal stability of nanostructured superhard coatings: A review,” *Surf. Coatings Technol.*, vol. 201, no. 13, pp. 6136–6142, Mar. 2007.

[21] J. Musil, “Hard nanocomposite coatings: Thermal stability, oxidation resistance and toughness,” *Surf. Coatings Technol.*, vol. 207, pp. 50–65, Aug. 2012.

[22] C. Mitterer, P. H. Mayrhofer, and J. Musil, “Thermal stability of PVD hard coatings,” *Vacuum*, vol. 71, no. 1–2, pp. 279–284, May 2003.

[23] Y. Long, J. Zeng, D. Yu, and S. Wu, “Microstructure of TiAlN and CrAlN coatings and cutting performance of coated silicon nitride inserts in cast iron turning,” *Ceram. Int.*, vol. 40, no. 7, pp. 9889–9894, Aug. 2014.

[24] N. Bagcivan, K. Bobzin, and R. H. Brugnara, “Investigation of the properties of low temperature (Cr 1-x Al x)N coatings deposited via hybrid PVD DC-MSIP/HPPMS,” *Materwiss. Werksttech.*, vol. 44, no. 8, pp. 667–672, Aug. 2013.

[25] T. Weirather, C. Czettl, P. Polcik, M. Kathrein, and C. Mitterer, “Industrial-scale sputter deposition of Cr1−xAlxN coatings with $0.21 \leq x \leq 0.74$ from segmented targets,” *Surf. Coatings Technol.*, vol. 232, pp. 303–310, Oct. 2013.

[26] N. Bagcivan, K. Bobzin, and S. Theiß, “(Cr1−xAlx)N: A comparison of direct current, middle frequency pulsed and high power pulsed magnetron sputtering for injection molding components,” *Thin Solid Films*, vol. 528, pp. 180–186, Jan. 2013.

[27] T. Polcar and A. Cavaleiro, “High-temperature tribological properties of CrAlN, CrAlSiN and AlCrSiN coatings,” *Surf. Coatings Technol.*, vol. 206, no. 6, pp. 1244–1251, Dec. 2011.

[28] R. Forsén, M. P. Johansson, M. Odén, and N. Ghafoor, “Effects of Ti alloying of AlCrN coatings on thermal stability and oxidation resistance,” *Thin Solid Films*, vol. 534, pp. 394–402, May 2013.

[29] A. Hörling, L. Hultman, M. Odén, J. Sjölén, and L. Karlsson, “Mechanical properties and machining performance of Ti1−xAlxN-coated cutting tools,” *Surf. Coatings Technol.*, vol. 191, no. 2–3, pp. 384–392, Feb. 2005.

[30] A. Flink, J. M. Andersson, B. Alling, R. Daniel, J. Sjölén, L. Karlsson, and L. Hultman, “Structure and thermal stability of arc evaporated (Ti0.33Al0.67)1−xSixN thin films,” *Thin Solid Films*, vol. 517, no. 2, pp. 714–721, Nov. 2008.

[31] C. Kirchlechner, K. J. Martinschitz, R. Daniel, M. Klaus, C. Genzel, C. Mitterer, and J. Keckes, “Residual stresses and thermal fatigue in CrN hard coatings characterized by high-temperature synchrotron X-ray diffraction,” *Thin Solid Films*, vol. 518, no. 8, pp. 2090–2096, Feb. 2010.

[32] F. Rivadulla, M. Bañobre-López, C. X. Quintela, A. Piñeiro, V. Pardo, D. Baldomir, M. A. López-Quintela, J. Rivas, C. a. Ramos, H. Salva, J.-S. Zhou, and J. B. Goodenough, “Reduction of the bulk modulus at high pressure in CrN,” *Nat. Mater.*, vol. 8, no. 12, pp. 947–951, Oct. 2009.

[33] P. C. Wo, P. R. Munroe, Z. Li, Z. T. Jiang, Z. H. Xie, Z. F. Zhou, and K. Y. Li, “Factors governing the mechanical behaviour of CrSiN coatings: Combined nanoindentation testing and transmission electron microscopy,” *Mater. Sci. Eng. A*, vol. 534, pp. 297–308, 2012.

[34] R. B. Toby, B. H., & Von Dreele, “GSAS-II: the genesis of a modern open-source all purpose crystallography software package,” *J. Appl. Crystallogr.*, vol. 46, no. 2, pp. 544–549, 2013.

[35] S. Vepřek, “The search for novel, superhard materials,” *J. Vac. Sci. Technol. A Vacuum, Surfaces, Film.*, vol. 17, no. 5, p. 2401, 1999.

[36] S. M. Aouadi, K. C. Wong, K. A. R. Mitchell, F. Namavar, E. Tobin, D. M. Mihut, and S. L. Rohde, “Characterization of titanium chromium nitride nanocomposite protective coatings,” *Appl. Surf. Sci.*, vol. 229, no. 1–4, pp. 387–394, May 2004.

[37] J. Musil and S. Kadlec, “Composite TiN – Ni thin films deposited by reactive magnetron sputter ion-plating,” vol. 110, no. 1998, pp. 168–172, 2000.

[38] T. Minami, S. Nishio, and Y. Murata, “Periodic microstructures of Cr–O–N coatings deposited by arc ion plating,” *Surf. Coatings Technol.*, vol. 254, pp. 402–409, 2014.

[39] Y.-C. Lu, S. Agnew, R. Dieckmann, and S.L. Sass, “Further characterization of the Aluminum peroxide oxide, AlO_2, formed by interfacial reaction between Pt and α-Al_2O_3,” *Acta Metall. Mater.*, vol. 43, no. 5, pp. 1885-1893, 1995.